Development of a Phase Diagram to Control Composite Manufacturing using Raman Spectroscopy

Stuart Farquharson[a], Jessica Carignan[a], Victor Khitrov[a], Antonio Senador[b], Montgomery Shaw[b]
[a]Real-Time Analyzers, 87 Church Street, East Hartford, CT 06108
[b]Institute of Material Science, University of Connecticut, Storrs, CT 06269

ABSTRACT

Fiber reinforced epoxy resins manufactured in autoclaves are expected to continue to dominate the composites market through 2010. However, the ability to obtain consistent mechanical properties from product-to-product remains difficult. This is largely due to the inability to monitor and control epoxy cure, loosely defined as the process of chain extension and cross-linking. Current autoclave process control employs a heat schedule based on a time-temperature-transformation (TTT) phase diagram that is determined by dynamic mechanical rheology. The phase diagram defines epoxy cure in terms of gelation and vitrification. We have been using an FT-Raman spectrometer to develop correlations between molecular (chain extension and cross-linking) and macroscopic (gelation and vitrification) data. The basis of a TTT phase diagram using Raman kinetic data for process control is presented for several reactions.

Keywords: TTT diagram, epoxy composites, Raman spectroscopy, process control

1. INTRODUCTION

The superior engineering properties of fiber-reinforced polymer matrix composites, primarily the high strength-to-weight ratio, make them highly desirable in aerospace applications (aircraft and rocket components).[1-3] Thermoset composites are primarily manufactured in two steps: preparing a prepreg and molding the part. Prepregs are prepared from a woven sheet of reinforcement fiber (carbon, glass or aramid) pre-impregnated (prepreg) with one or more matrix components (usually a partially cured thermoset polymer or thermoplastic). The prepreg is then shaped and cured in a combination heat and molding device (e.g. autoclave), and cured according to the manufacturer's schedule.[4] This schedule is based on pre-determined, off-line measurements such as dynamic mechanical rheology.[5] The isothermal cure of a thermoset resin can be characterized in terms of gelation and vitrification. Gelation is generally defined as the transformation of the resin from the liquid to rubbery state, while vitrification is the transformation from the rubbery state to the glass state. Gelation and vitrification experiments are often used to develop a time-temperature-transformation (TTT) diagram. Essentially, a series of rheology measurements are performed at various isothermal cure temperatures. The gel and vitrification times can be calculated from the measured storage (G') and loss moduli (G"), as a maximum in G" and a maximum in G"/G', respectively.[6,7] Vitrification follows an S-shaped curve in the TTT diagram due to the chemical kinetics (which increase with temperature) and the physical changes that slow the reaction (e.g. increasing molecular weight). For a given isothermal cure, the vitrification point represents the cessation of reaction, as the increased viscosity and/or molecular weight prevent further reactive group interactions. A generalized diagram developed for the cure of diglycidyl ether of bisphenol A (DGEBA), the most widely used thermoset, by triethyltetraamine (TETA), a typical amine, is shown in Figure 1.[8]

Ideally, the TTT diagram aids a manufacturer in selecting a heat schedule to produce a cured resin with the desired properties. The temperature at which gelation occurs, Tg_{gel}, is a very useful parameter, in that a resin cured below this temperature will predominantly contain long-chains and will be more pliable, whereas above this temperature the converse is true (higher cross-linking, more rigid). The S-shaped vitrification curve can be used to select a cure temperature to prepare a composite with the desired extent-of-cure and toughness.[9,10] Nevertheless, even with a well developed TTT diagram, consistent fabrication of components within specifications has proven difficult, and has led to high production costs.[11,12] This is often attributed to slight variations in the pre-polymer formulations that can influence reaction mechanisms. For example, a prepreg that has matured during storage may have a higher than usual content of pre-extended base resin. This would decrease the amount of cross-linking for a pre-selected cure temperature resulting in a product that is more pliable than desired. Also, the TTT diagram is only valid for isothermal cures, and manufacturing practices usually include temperature ramps.

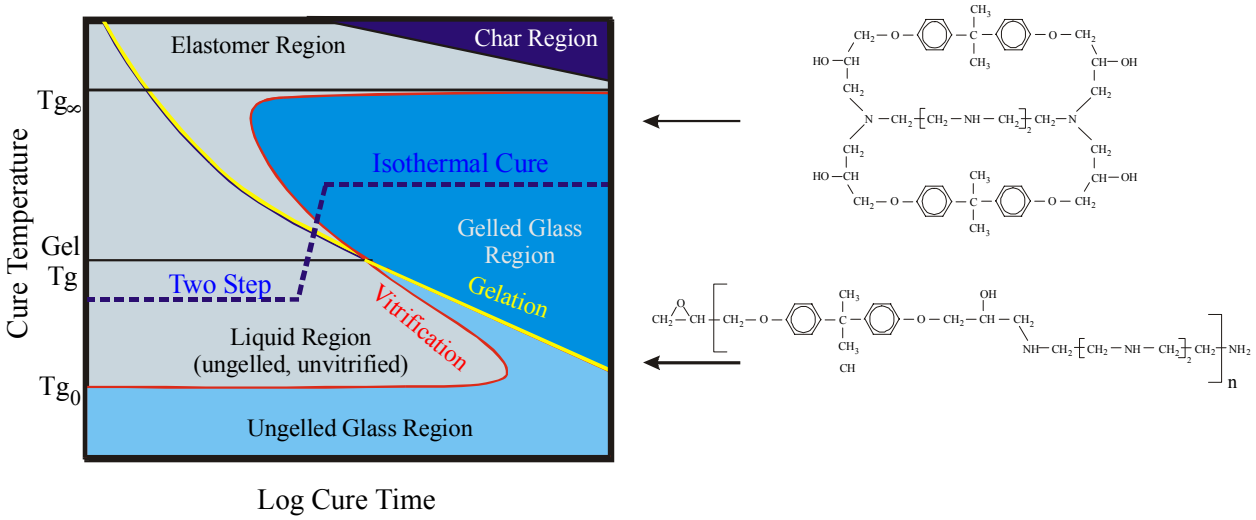

Figure 1. Generalized Time-Temperature-Transformation phase diagram based on isothermal cure of DGEBA with TETA. Note regions and gelation and vitrification curves. Chemical structures are included to indicate the extreme cases of predominantly cross-linked (top) and chain extension (bottom). TTT diagram redrawn from Reference 8.

It is generally recognized that optimized process control with minimum waste will require: a sensor to collect real-time process data (preferably molecular *and* macroscopic), a cure model based on reaction mechanisms, correlations between molecular structure and properties, and an expert system to control the fabrication device.[1] In recent years, researchers have been investigating fiber optic based spectroscopies to monitor polymer and composite cure in real-time. This includes fluorescence,[13,14] near infrared,[15] infrared[16] and Raman spectroscopies.[17,18] Raman measurements have been very successful at monitoring the cure of epoxy resins, and at least one measurement of composite cure has been performed in an industrial autoclave.[19] However, only limited studies employing infrared,[8] nuclear magnetic resonance,[20] and Raman spectroscopy[21,22] have been performed to develop the necessary correlations between molecular kinetics and physical properties required to achieve process control. It is realized that the composite properties are due to the combined properties of the reinforcement fiber and the matrix material. However, the matrix properties can be greatly varied by the process conditions. In an effort to develop the required correlations we have integrated fiber optics into a parallel plate rheometer to collect Raman spectra simultaneous to rheological data. Here we present simultaneous measurements during the cure of three epoxy resin systems.

2. EXPERIMENTAL

Diglycidyl ether of bisphenol A (DER 331), dipropylene glycol diglycidyl ether (DER 736), triethyltetraamine (TETA), and ethyldiamine (EDA) were obtained from the Dow Chemical Company (Midland, MI) and used without modification. These reactants were used to perform three reactions, DER 331 cured with TETA, DER 331 cured with EDA, and DER 736 cured with TETA. These epoxy curing reactions were first monitored in a small isothermal laboratory reactor in order to identify the Raman spectral features associated with primary and secondary amine reactions, chain extension and cross-linking reactions, kinetic relationships, and rate constants. The laboratory reactor consisted of a ½" diameter by ½" deep hole machined into a 1x3x4" aluminum block and fit with computer controlled cartridge heaters. An aluminum foil cup was filled with the reactants and fit into the aluminum block pre-heated to the desired temperature. A downward looking probe, used to excite the sample and collect the Raman scattering, was placed such that the focal point was just below the sample surface. The probe contained a notch filter to remove silica bands and an f/0.7 aspheric lens that focused the beam into the sample and collected the scattered radiation back along the same axis. A dichroic filter (Omega Optical, Brattleborough, VT) was used to reflect the excitation laser to the lens and pass the Raman scattered radiation collected by the lens. An f/2 achromat was used to collimate the laser beam exiting a 200 µm core diameter source fiber optic, while a second f/2 achromat was used to focus the scattered radiation into a 365 µm fiber optic (Spectran, Avon, CT). A short pass filter was placed in the excitation beam path to block the silicon Raman scattering generated in the source fiber from reflecting off sampling optics and reaching the detector. A long

pass filter was placed in the collection beam path to block the sample Rayleigh scattering from reaching the detector. A Fourier transform Raman spectrometer was used to deliver 100 to 500 mW of power to the sample (Real-Time Analyzers, model IRA-785, East Hartford, CT).

A LabVIEW (National Instruments, Austin, TX) program was written that displayed each spectrum as it was collected. The program also allowed selecting a spectral feature (peak height, integrated area, or region), correcting it for baseline offsets (linear), normalizing it to another feature, and plotting it as a function of cure time. Once the experiment was complete, the data could be fit to a model to determine a rate constant.

A Rheometric Scientific ARES (Advanced Rheometric Expansion System) parallel-plate rheometer was used for simultaneous physical and chemical property measurements. The parallel plates were 34 mm in diameter and the upper one was machined to allow insertion of the fiber optic probe (Figure 2). The hole was angled at 20^{o} off normal to the surface to minimize reflection of the laser into the collection fiber optics. The probe tips were encased in a stainless steel ferrule and a set screw held each in place. The probe tip contained six collection fibers around a single excitation fiber, all of which were 200 μm in diameter. The other end of the 8-foot long fiber optic probe was bifurcated and connected to the source laser and the Raman instrument. A blocking filter (788 AGSP, Omega Optical, Brattleboro, VT) was placed between the laser and the source fiber to remove excessive laser radiation that would contribute to the Raman spectra. Only 200 mW of the 785 nm excitation laser reached the sample. Typical of this probe design, the Raman spectra contained a significant silica contribution from the source fiber. The samples were mixed at room temperature and placed between the parallel plates of the modified ARES rheometer. The rheometer was used to isothermally heat the samples, while a servo motor supplied an oscillating, torsional strain to the upper plate and the response was measured by a transducer in the lower plate as torque or stress. The strain was automatically adjusted between 0.3 and 50% to maintain the torque within the optimum signal range (1 to 10 rad/s). The strain, torque and the response lag time (δ) were used to calculate the elastic (storage) modulus and the viscous (loss) modulus (G' and G", respectively). These values were in turn used to calculate the gel time (G'= G") and the vitrification time (dtanδ/dt = 0). In all experiments, the parallel plate rheometer was run in the *autostrain* mode with a *constant static force* to perform a *Dynamic Time Sweep*, and temperatures varied by 1 or 2 ^{o}C from preset values.

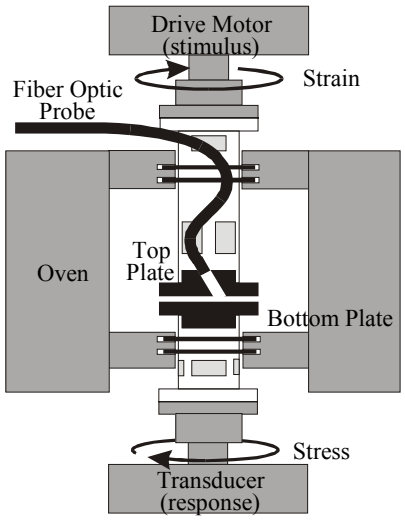

Figure 2. Schematic of a parallel-plate rheometer (including fiber optic probe

3. RESULTS AND DISCUSSION

Since the most widely used composite matrix material is epoxy resin formed from DER 331 cured by TETA, this epoxy was used for the initial studies. The basic chemical reaction is shown in Figure 3, while representative Raman spectra of the uncured and cured epoxy at 70 ^{o}C are shown in Figure 4. The Raman bands of interest are numbered, as are the corresponding functional groups. In all cases, the reactants were first mixed at room temperature, and then placed into the laboratory reactor. In this example, a 3:1 DER 331 to TETA molar ratio was used such that an equivalent amount of epoxy ring and amine functional groups were available for reaction. It can be seen that numerous Raman bands changed intensity as the reaction progressed, while others did not. The latter included bands at 394, 643, 739, 826, 941, 1016, 1117, 1190, 1586, 1612, 2934, and 3070 cm^{-1}. The phenyl ring stretch (1) and phenyl-hydrogen stretch (2) do not participate in the reaction, and their Raman bands at 1612 and 3070 cm^{-1} maintain constant intensity, and can be used as internal intensity standards to normalize the intensity of all other bands. The following bands *decreased* in intensity as the reaction progressed, 668, 766, 918, 986, 1160, 1256, 1347, and 3010 cm^{-1}. The Raman bands at 1256 and 3010 cm^{-1} correspond to the oxirane (3) and its methylene stretch (4) and are ideal to monitor the opening of the ring during reaction. The following *increased* intensity during reaction, 1464, 2837, 2875, and 2965 cm^{-1}, while new bands appeared at 2716 and 2763cm^{-1}. The two methylene deformation (5) modes associated with DER 331 and TETA occur at 1450 and 1464 cm^{-1}, but are not differentiated. The corresponding stretching modes (6) appear to coincide at 2875

cm^{-1}. During reaction methylene bridges are formed linking the two reactants, and the deformation mode (7) Raman band increases intensity and shifts to 1467 cm^{-1}, while the stretching mode (8) Raman band at 2875 cm^{-1} increased in intensity. Symmetric (9) and asymmetric (10) methyne modes formed by the reaction also appear at 2716 and 2763 cm^{-1}, respectively.

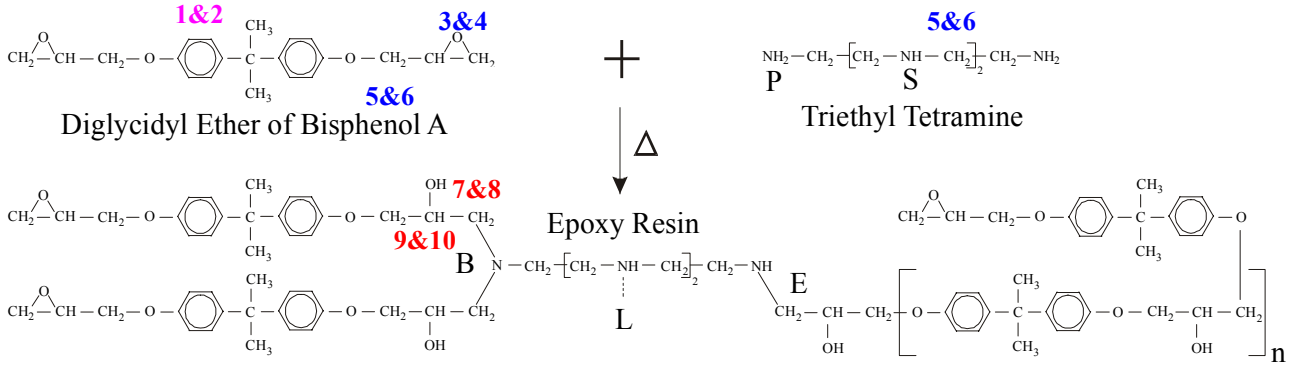

Figure 3. Chemical structures and cure reaction of DGEBA by TETA. Possible reaction mechanisms include the epoxy oxirane with 1) the primary amine (P) resulting in chain extension (E), 2) the newly formed secondary amine resulting in branching (B) or 3) the mid-molecule secondary amines resulting in cross-linking (XL).

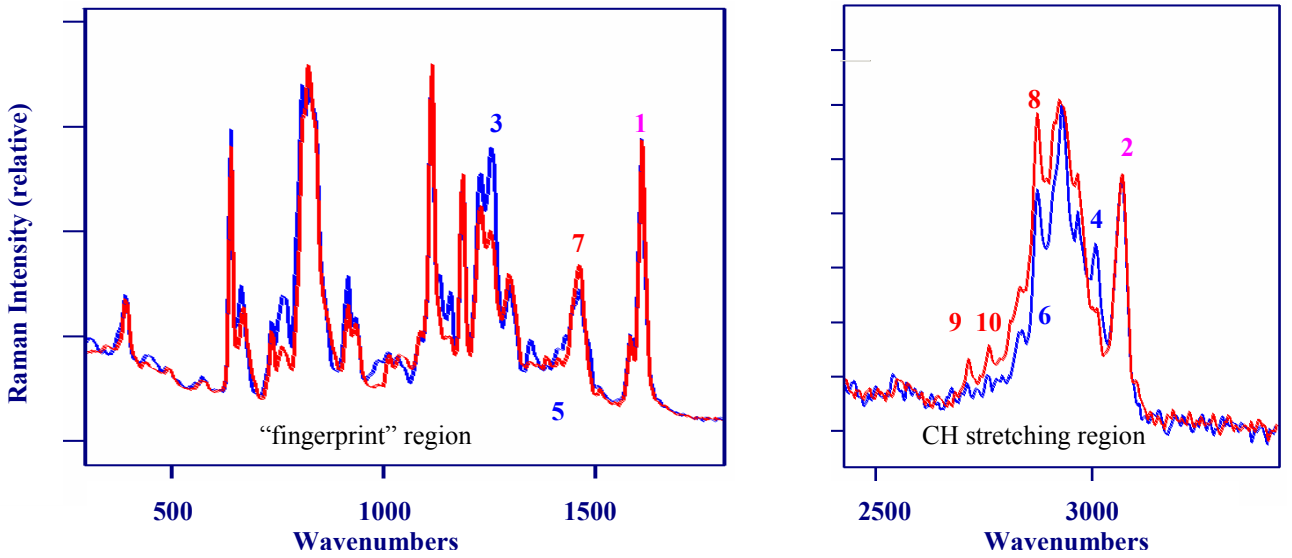

Figure 4. Raman spectra of uncured and cured DER 331 and TETA at 70 °C (first spectra - blue, and last spectra - red). Molecular vibrations and corresponding Raman modes are numbered. Conditions: 500 mW of 785 nm, 8 cm^{-1}, 50 scans (1.5 min).

Kinetic studies were performed for DER 331 cured by TETA at 40, 50 and 70 °C. In all cases each of the bands described above were plotted as a function of temperature and fit with rate equations. This was accomplished by first applying a baseline offset (the RMS value between 2400-2500 cm^{-1} was subtracted from the entire spectrum), normalizing each spectrum to the 1612 cm^{-1} band intensity, measuring the band intensity, I, as height or area for each sequential spectra, normalizing the intensity from 0 to 1 for the entire time sequence, then iteratively optimizing the constants A, B and C for the following equation:

$$I = A\text{-}Be^{-Ct^d} \qquad \text{Equation 1}$$

where C is the rate constant, and d =1 or 2. In general, all bands yielded similar rate constants. In the case of isothermal cure at 50 °C, both the decrease in the band at 1256 cm^{-1} due to breaking of the oxirane (3), and the increase of the band at 2875 cm^{-1} due to the formation of the methylene bridge (8) have identical decay and formation rate constants of 1.85 $x10^{-3}$ I_{Raman}/min^2 (Figure 5). As shown, the data for each band had different amounts of scatter that is attributed to the

relative intensity of the bands and/or overlap with adjacent bands. The time-squared term in this rate equation, sometimes referred to as a stretched-exponential, requires comment. Early studies of epoxy cure by Raman spectroscopy typically fit the disappearance of the oxirane mode at 1256 cm^{-1} with a simple first-order decay (i.e. d = 1 above).[18] A more recent study fit the shift of the CH stretching Raman bands as a group to lower frequencies with the stretched exponential decay (d=2).[23] The latter data was collected using 1064 nm laser excitation, and the inferior response of the InGaAs detector did not allow fitting the 1256 cm^{-1} oxirane band reliably. Nevertheless, that study attributed the time-squared term to the formation of a termolecular intermediate, in which the hydroxyl group formed by the reaction of the primary amine catalyzes the reaction of the newly formed secondary amine. The stretched-exponential behavior has also been reported for epoxy systems studied by near-infrared spectroscopy,[24] while the termolecular intermediate has previously been suggested.[25]

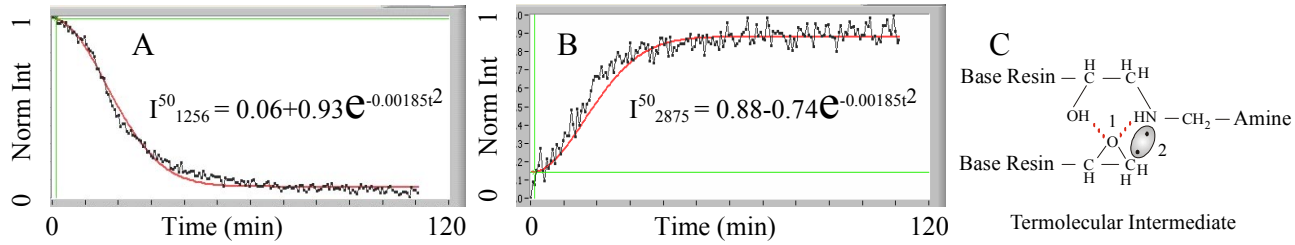

Figure 5. Plots of normalized band intensities for A) 1256 cm^{-1} and B) 2875 cm^{-1} for DER331 cured by TETA at 50 °C. Stretched-exponential reaction equations are fit to both sets of data with identical rate constants. Conditions as in Figure 2, but 0.5 min acquisition time per spectrum. C) Termolecular intermediate, hydrogen bonding (• • •) and electron pair shown.

The second reaction studied also employed DER 331 as the base epoxy, but used EDA as the curing agent. EDA was selected because it does not contain any mid-molecule amines, and no cross-linking is expected, which should yield a product that contains a significantly higher amount of chain-extension. However, it should be noted that the structural distinction between branching and cross-linking, as defined by Figure 1, is subtle. Furthermore, since EDA has only primary amines, they represent the initial reactions, and secondary amine reactions follow. For this reaction, a 2:1 DER 331 to EDA molar ratio was used. Representative Raman spectra of the uncured and cured epoxy at 30 °C are shown in Figure 6. As in the previous reaction, numerous Raman bands changed intensity as the reaction progressed, while others did not. The latter included bands at 394, 739, 826, 941, 1016, 1117, 1190, 1586, 1612, 2934, and 3070 cm^{-1}. Again the 1612 cm^{-1} band was used as an internal intensity reference standard. The following bands decreased in intensity as the reaction progressed, 465, 668, 766, 810, 918, 986, 1160, 1256, 1347, and 3010 cm^{-1}, while the following increased intensity, 1462 and 2875 cm^{-1}.

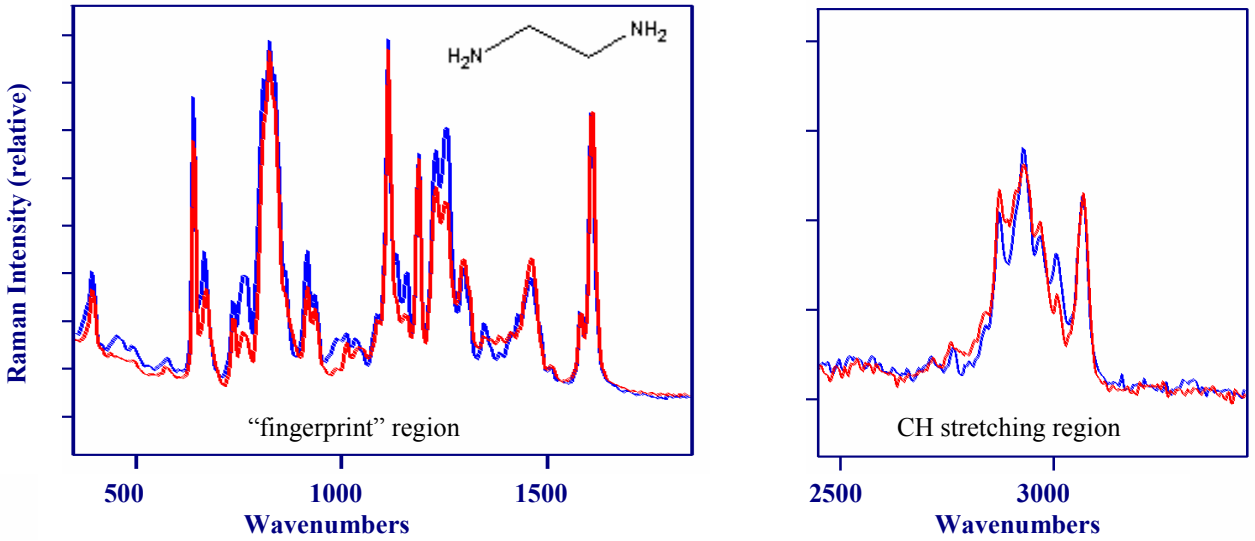

Figure 6. Raman spectra of uncured and cured DER 331 and EDA (structure in inset) at 30 °C (first spectra - blue, and last spectra - red). Conditions as in Figure 2.

As expected, the bands that change intensity are best fit with a stretched-exponential decay or growth rate. For example, the decrease in the band at 1256 cm^{-1} due to breaking of the oxirane (3) has a decay rate constant of 4.55 $x10^{-4}$ I_{Raman}/min^2 at 40 °C (Figure 7A). However, for this reaction, the band at 465 cm^{-1} is best fit with a first-order decay rate equation (Figure 5B). Bands at this low frequency are typically due to backbone stretches, and since the band appears in the pure EDA spectrum, it is assigned to the N-C-C-N stretch. Any reaction will disrupt this mode, and its rapid, first-order disappearance, at a significant faster rate than the oxirane mode, suggests it is associated with the primary amine reaction. Although the 465 cm^{-1} band also disappears at a faster rate in the previous reaction using TETA as the curing agent, the scatter in the data was too large to reliably fit a rate equation.

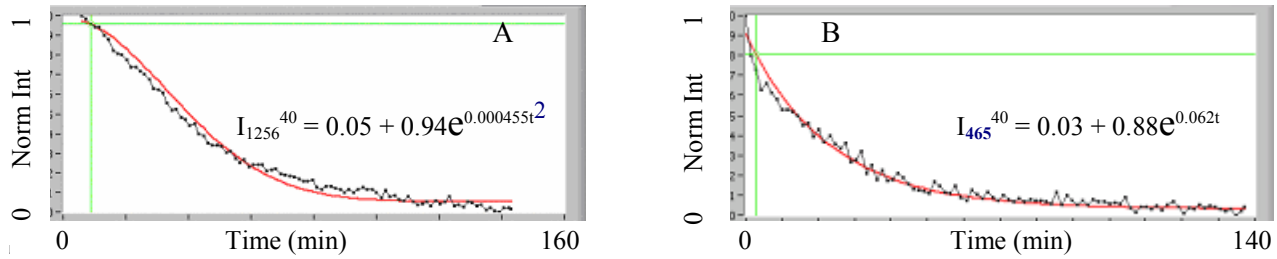

Figure 7. Plots of normalized band intensities for A) 1256 and B) 465 cm^{-1} for DER331 + EDA at 40 °C. Conditions as in Figure 3.

The third reaction employed DER 736 as the base resin and TETA as the curing agent. DER 736 was selected because it does not contain phenyl rings and should produce a more pliable product. For this reaction, a 3:1 DER 736 to TETA molar ratio was used. Representative Raman spectra of the uncured and cured epoxy at 70 °C are shown in Figure 8. As in the previous reactions, numerous Raman bands changed intensity as the reaction progressed, while the bands at 709, 854 and 2935 cm^{-1} did not. The latter band, the asymmetric CH_2 stretch, was used as the internal intensity reference standard. The bands at 753, 914, 990, 1137, 1260, and 3000 cm^{-1} decreased intensity, while the bands at 1305, 1460, 2876, and 2965 cm^{-1} increased intensity as the reaction progressed. For this reaction, it was found that only at the highest cure temperature measured, 80 °C, does the reaction follow the stretched-exponential rate, otherwise, the data is best fit with a first order exponential equation (Figure 9). This suggests that at low temperatures, the termolecular intermediate does not form, and further suggests that the phenyl rings in DER 331 may be required to sterically align the epoxy with the secondary amine and hydroxyl group. The cure data for the 80 °C cure reaction also shows departure from a pure stretched-exponential equation, which may represent a contribution from a reaction that has a high activation energy. One possibility is the reaction between the oxirane and the formed hydroxyl group, which has been postulated to occur at high temperatures.[25] More detailed analysis of this and related reactions are required to substantiate the suggested steric alignment mechanism and the hydroxyl reaction.

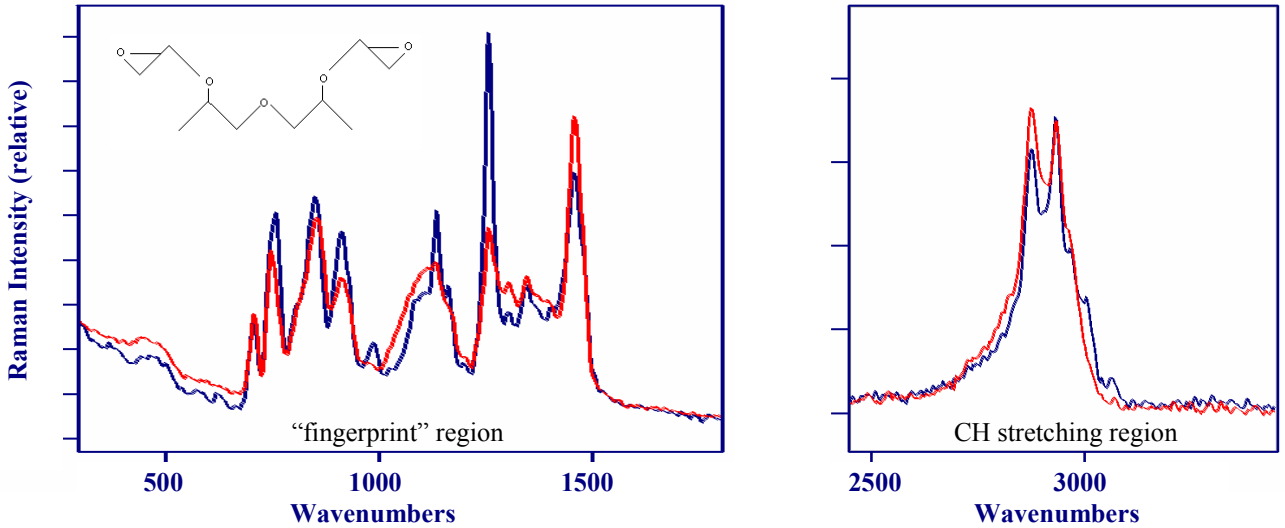

Figure 8. Raman spectra of uncured and cured DER 736 (structure in inset) and TETA at 70 °C (first spectra - blue, and last spectra - red). Conditions as in Figure 2, but 0.5 min acquisition time.

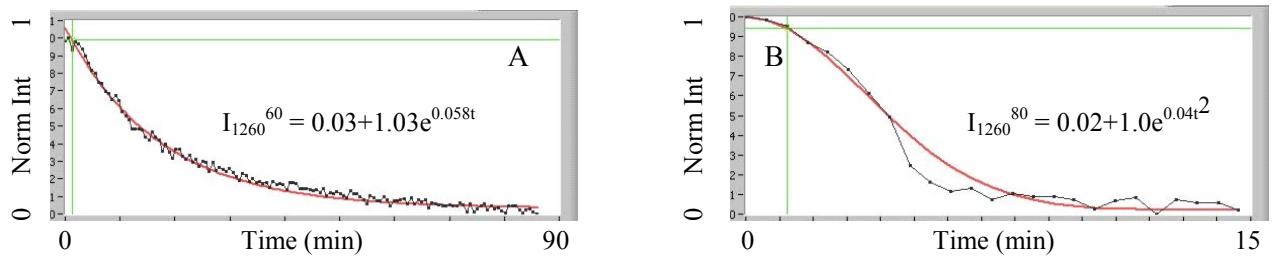

Figure 9. Plots of normalized band intensities for 1256 cm^{-1} for DER 736 cured by EDA at A) 60 °C and B) at 80 °C. Conditions as in Figure 2, but 0.5 min acquisition time per spectrum.

The first simultaneous rheology and Raman measurements were performed using DER 331 cured by TETA. Isothermal cure was performed at 30, 35, 40, 45, 50, 55, 60, 65, and 70 °C. Based on the laboratory reactor studies, the Raman kinetics were determined using the band intensity of the oxirane mode at 1256 cm^{-1} referenced to the phenyl trigonal ring-stretching mode at 1612 cm^{-1}. In all cases the data could be fit with a stretched-exponential, and the rate constants as a function of temperature are listed in Table 1. The rate constants were then used to calculate the activation energy, Ea for the observed reaction according to the Arrhenius equation:

$$k = Ae^{-Ea/RT} \qquad \text{Equation 2}$$

where A is a constant, R is the ideal gas constant (8.3144 J/K•mole) and T is absolute temperature (Table 1). A plot of Ln k vs. 1000/T for the rheological Raman data yields a slope (Ea/R) of 16.2 corresponding to an activation energy of 134.7 kJ/mole (Figure 10). Adding the three laboratory reactor rate constants to this data show the experiments to be in good agreement.

Representative rheology data is shown in Figure 11 for DER 331 cured by TETA at 60 °C. The plates were oscillated at a frequency of 6.28 rad/s, with a maximum applied strain of 10% and allowed torque of 20.0 g·cm, with data collected every 10 sec. The vitrification time was taken as the maximum value of tan δ, while the gelation time was taken as the crossover point of the storage and loss moduli. Here the vitrification point is ~ 10 min, while the gel point is more precisely defined at 21.7 min. Similar to the Raman rate constants, an activation energy was determined by plotting the natural log of the gelation and vitrification times as a function of 1000/T (Figure11B). The activation energy for gelation is found to be 80.2 kJ/mole, while the activation energy for vitrification is 62.2 kJ/mole, both considerably lower than the Raman activation energy of 134.7 kJ/mole.

Table 1. Parameters to calculate Ea for DER 331 cured by TETA. Lab reactor values (3) are at the top (bold), rheometer are at the bottom.

T (oC)	k	Ln k	Abs Ln k	1000/T (K)
40	**3.25E-04**	**-8.03**	**8.03**	**3.19**
50	**1.85E-03**	**-6.29**	**6.29**	**3.10**
70	**3.55E-02**	**-3.34**	**3.34**	**2.92**
35	1.47E-04	-8.83	8.83	3.25
40	3.30E-04	-8.02	8.02	3.19
45	8.60E-04	-7.06	7.06	3.14
50	1.25E-03	-6.68	6.68	3.10
55	2.70E-03	-5.91	5.91	3.05
60	7.70E-03	-4.87	4.87	3.00
65	1.32E-02	-4.33	4.33	2.96
70	3.70E-02	-3.30	3.30	2.92

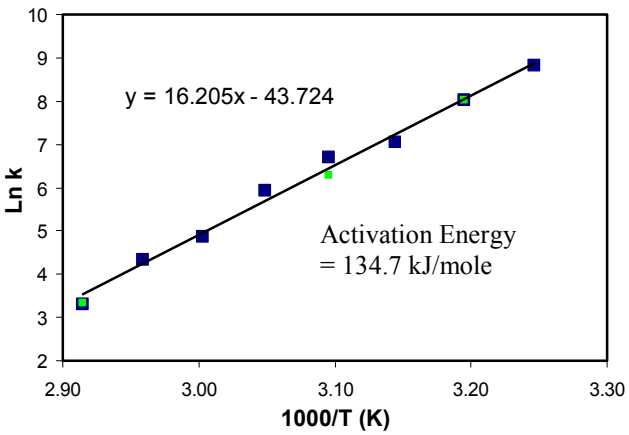

Figure 10. Plot of Ln k vs 1000/T (K) for DER 331 cured by TETA. Slope times R yields Ea. Lab (■) and rheometer (■) data combined.

The simultaneous Rheology and Raman data for the cure of DER 331 by EDA duplicated the previous reaction, in that isothermal cure was performed at 30, 40, 45, 50, 55, and 60 °C, the intensity of the 1256 cm^{-1} band referenced to the 1612 cm^{-1} band was used to determine rate constants using stretched-exponential rate equations, these rate constants and those determined in the laboratory reactor were used to calculate the activation energy for this reaction (Figure 12A).

However, here the calculated activation energies in the rheometer and the laboratory reactor were slightly different at 110.6 and 102.9 kJ/mole, respectively.

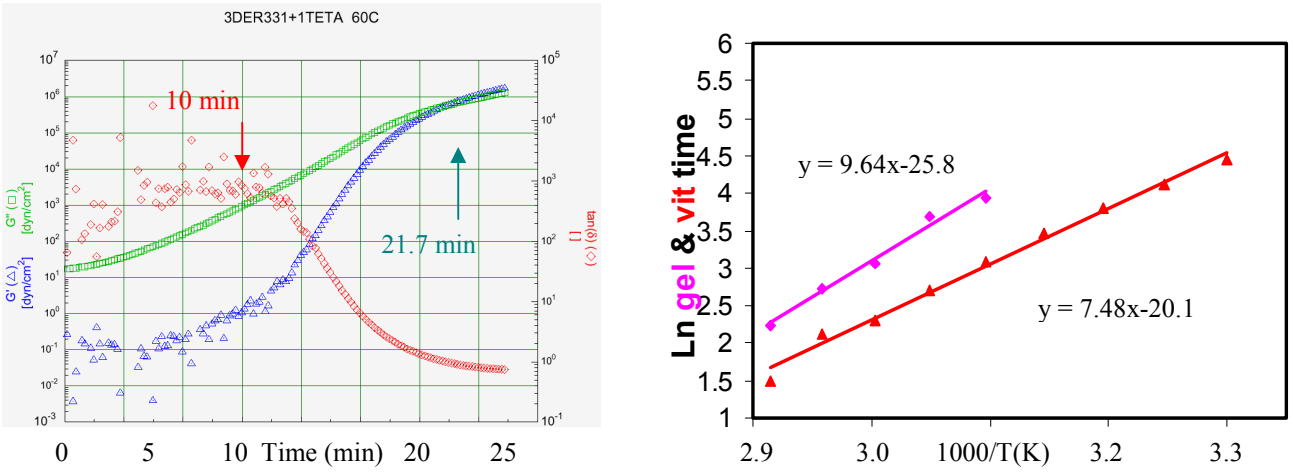

Figure 11. A) Measured storage (G') and loss (G") moduli and calculated tan δ (G"/G') as a function of cure time for DER331 + TETA at 60 °C. 34 mm diameter plates at a 2.1 mm gap. B) Plot of Ln gelation (♦) and vitrification (▲) time vs 1000/T (K) for DER 331 cured by TETA.

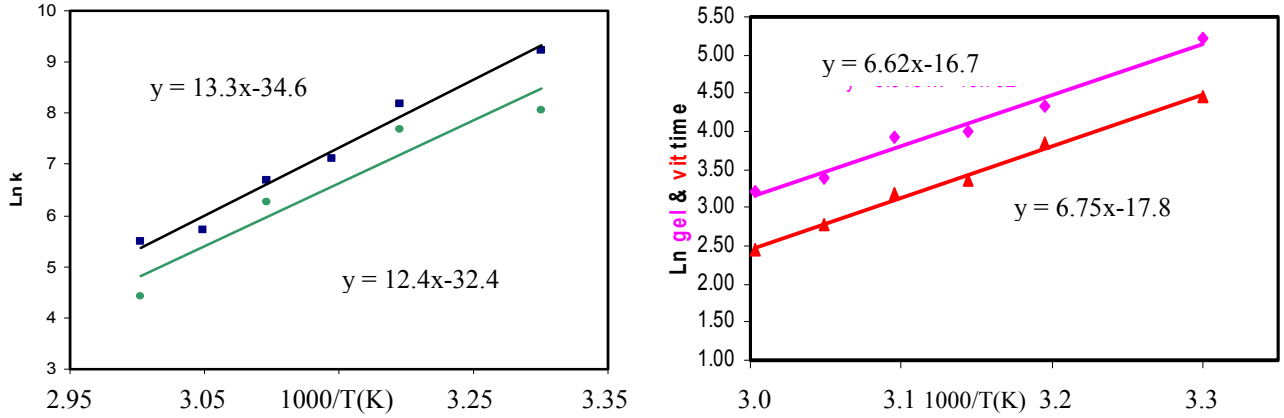

Figure 12. A) Plot of Ln k vs 1000/T (K) for DER 331 cured by EDA. Lab reactor (■) and rheometer (■) data combined. B) Plot of Ln gelation (♦) and vitrification (▲) time vs 1000/T (K), rheometer data.

The vitrification and gelation times were also determined as previously described and used to calculate corresponding activation energies of 56.1 and 54.9 kJ/mole, respectively (Figure 12B). Again these values are considerably lower than the Raman activation energy of ~107 kJ/mole. Furthermore, both the rheometer and Raman activation energies were lower for this reaction, than cure with TETA. This is consistent with the fact that by using EDA and eliminating cross-linking reactions, the overall cure reaction requires less energy.

The simultaneous Rheology and Raman data for the cure of DER 736 by TETA also duplicated the previous reactions, in that isothermal cure was performed at 40, 50, 60, 65, 70 and 80 °C; the intensity of the 1256 cm^{-1} band referenced this time to the 2935 cm^{-1} band was used to determine rate constants using first-order rate equations; and these rate constants and those determined in the laboratory reactor were used to calculate the activation energy for this reaction (Figure 13A). Here the calculated activation energies in the rheometer and the laboratory reactor were slightly different at 54.9 and 60.6 kJ/mole, respectively, while the activation energies determined from the vitrification and gelation times were similar at 62.2 and 51.2, respectively (Figure 13B).

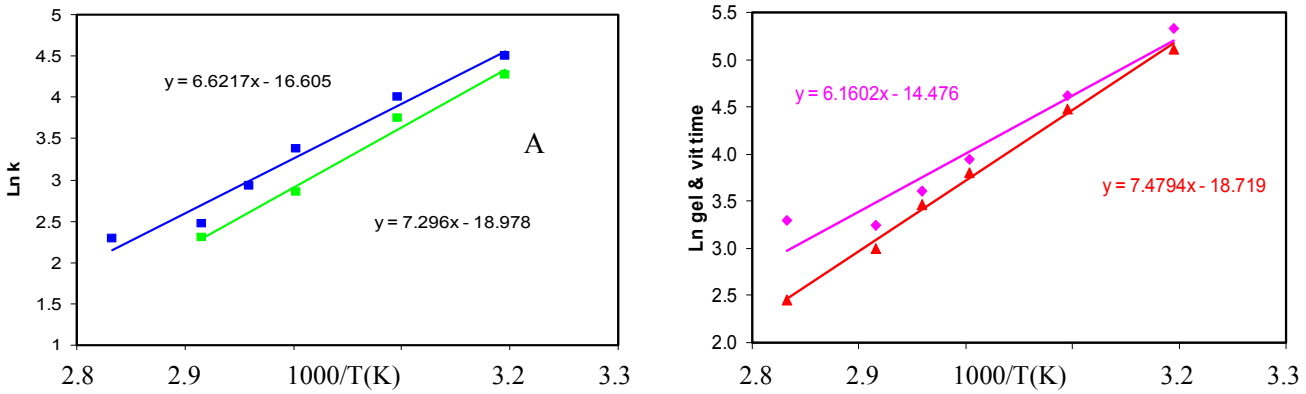

Figure 13. A) Plot of Ln k vs 1000/T (K) for DER736 cured by TETA. Lab reactor (■) and rheometer (■) data combined. B) Plot of Ln gelation (♦) and vitrification (▲) time vs 1000/T (K), rheometer data.

As stated, a time-temperature-transformation phase diagram is a useful model to determine the heat schedule required to manufacture a product with the desired properties. The rheology data is incorporated into a TTT phase diagram by plotting the gel and vitrification data cure temperatures as a function of log cure times. The gel and vitrification times represent physical changes in the epoxy that indicate near completion of the reaction. For the Raman data, a time when the reaction reaches 90% completion is used (I=0.1). This is determined by solving for **t** in Equation 3, i.e.;

$$\mathbf{t}(\text{min}) = [(\ln(1/0.1)/\mathbf{k}]^{1/d} \qquad \text{Equation 3}$$

where d is 1 for first-order and 2 for stretched-exponential rate equations. All of the data falls in the lower right quadrant of the TTT diagram shown in Figure 1, and in general it was found that the Raman phase data falls in between the vitrification and gel data (Figure 14). In fact the Raman and gelation phase data are nearly identical suggesting a strong correlation, at least for these epoxy systems.

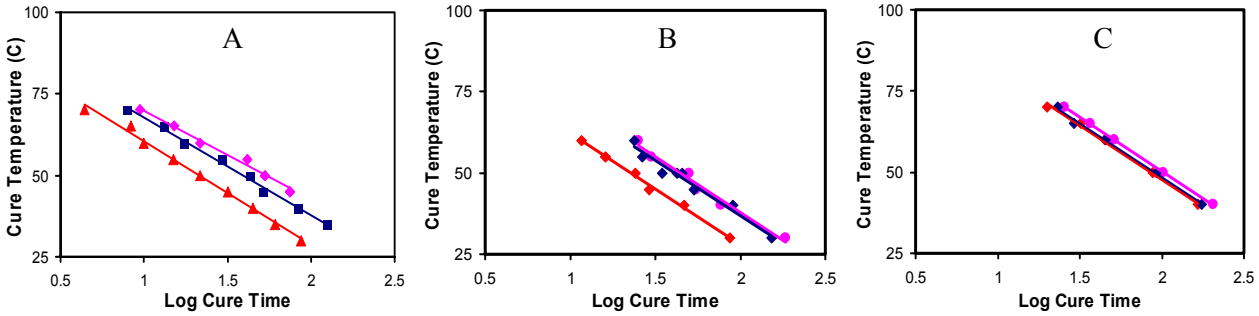

Figure 14. TTT phase diagram showing the correlation between gel time (♦), vitrification (▲) time, and 90% Raman cure time (■) for the following epoxy reactions A) DER 331 + TETA, B) DER 331 + EDA, and C) DER 736 + TETA.

The activation energies determined by both Raman spectroscopy and rheology for all three reactions are summarized in Table 2. It is clear that a reasonable correspondence between Raman and rheology activation energies only occurs for the reaction of DER 736 and TETA. Since this reaction was the only one that followed first-order kinetics, it suggested taking the stretched-exponential term into account, particularly in view of the above phase data. This results in a very close correlation between the activation energies determined by rheology and Raman spectral measurements.

Table 2. Comparison of activation energies determined by rheology and Raman spectral measurements.

	Activation Energy (kJ/mole)				
Reaction	Vitrification	Gelation	Raman	Raman/t_{exp}	Average Rheology
DER 331 + TETA	62.2	80.2	134.7	67.4	71.2
DER 331 + EDA	56.1	54.9	110.6	55.3	55.5
DER 736 + TETA	62.2	51.2	54.9	54.9	56.8

4. CONCLUSION

High quality kinetic data was obtained by employing a unique FT-Raman spectrometer that employed 785 nm laser excitation and silicon detection. The combination of wavenumber stability and improved sensitivity yielded spectra with high S/N in less than 1 minute. This in turn allowed precise fitting of the cure data with kinetic equations. It was shown that the reaction of DER 736 with TETA follows first-order kinetics, while the reaction of DER 331 with TETA follows autocatalytic kinetics. The latter kinetics confirm the existence of the postulated termolecular intermediate. While the reaction of DER 331 with EDA also followed autocatalytic kinetics, a Raman band at 465 cm^{-1} followed first-order kinetics. This band was assigned to an EDA backbone stretch and its change in intensity to the reaction of the primary amine. Although this band could be assigned to chain extension, no obvious Raman band, as yet, could be distinctly assigned to cross-linking.

The collection of Raman spectral data simultaneous with rheological data allowed developing correlations between molecular and macroscopic properties. Once the stretched-exponential term in the Raman kinetic data was taken into account, the activation energies measured by Raman spectroscopy and rheology were equivalent within experimental error for all three reactions studied. Consideration of the fact that gelation and vitrification represent the time when a reaction nears completion, suggested comparing the time that the Raman kinetic data indicates that 90% of the reaction is complete. It was shown that the 90% cure time determined by Raman spectroscopy and the gelation time determined by rheology were nearly identical over the temperature range studied. Furthermore, time-temperature-transformation phase diagrams were made for each reaction showing that this 90% cure time could be used equally as the gel times to define the phase transition from liquid to gelled state. The diversity of the epoxy systems studied lends credibility to these correlations, and a Raman-based TTT phase diagram might form the basis of a molecular model to select a cure schedule (time-temperature). Finally, the ability to use the same method (Raman spectroscopy) to monitor molecular changes in real-time within manufacturing devices suggests real-time process control of thermoset-based composites.

ACKNOWLEDGEMENTS

The authors are grateful to the U.S. Missile Defense Agency for supporting this work (Contract Number DASG60-02-P-0156).

REFERENCES

1 Jang, B.Z., Advanced Polymer Composites: Principles and Applications of Fibers, ASM International, (1994)
2 Lee, H. and K. Neville , Handbook of Epoxy Resins, McGraw Hill Book Company, New York, NY, (1982).
3 Dickie, R.A., S.S. Labana, and R. S. Bauer, Cross-linked Polymers: Chemistry, Properties, and Applications, Ed., ACS Symposium Series 367 (1988)
4 For example, see product literature from Dow Chemical (Midland, MI), Fiberite (Tempe, AZ), or Hexcel (Pleasonton, CA)
5 Bidstrup, W.W. and S.D. Senturia, "Monitoring the cure of a composite matrix resin with microdielctrometry", *Polym. Eng. Sci.*, 29, 290-294 (1989)
6 Ross-Murphy, S.B. “Rheological Characterization of Gels”, *J. Texture Studies*, 26, 391-400 (1995)
7 Tung, C.M., and Dynes, P.I.J. *J. Applied Polymer Science*, 27, 4569-574 (1982)
8 Enns, J.B. and J.K. Gillham, "Time-Temperature-Transformation Cure Diagram: Modeling the cure behaviour of thermosets:, *J. Applied Polymer Science*, 28, 2567-2591 (1983)
9 Allcock, H.R. and F.W. Lampe, Contemporary Polymer Chemistry, Prentice Hall, Englewood Cliffs, NJ, Chapter 21 (1981)
10 Sinclair, R.A., Ultrastructure Processing of Ceramics, Glasses, and Composites, (Hench, L.L. and Ulrich, D.R., Eds) John Wiley & Sons, New York, NY, 256-264 (1984)
11 Benjamin, B., *High-Performance Composites*, 21-22 (1993)
12 Wilson, D., “PMR-15 Processing, Properties and Problems – A Review”, *British Polymer Journal*, 20, 405-416 (1988)
13 Fuchs, A., Paix, H.J., and Sung, N.-H., *ANTEC*, "Epoxy Cure Monitoring at the Fiber/Matrix Interfaces Using Fiber Optic Evanescent Fluorimetry", 243-244 (1992)
14 Sun, X.-D. and Sung, C.S.P., *ACS Polym. Preprints*, 35(1), "Intrinsic Fluorescence Cure Sensor for Reaction Monitoring in Polyurethane", ACS, 435-436 (1994)

15 Farquharson, S., Arnoudse, P.B., Wyckoff, M.H. and Keillor, P.T., III., “On-Line Analysis of Extruded Polymers via Fiber Optic Coupled Fourier Transform Near-IR Spectroscopy” *SPIE*, 1172, 164-173 (1989)
16 Druy, M.A., Elandjian, L., Stevenson, W.A., Driver, R.D., Leskowitz, G.M., Curtiss, L.E., "Fourier Transform Infrared (FTIR) Fiber Optic Monitoring of Composites During Cure in an Autoclave," *SPIE*, Vol. 1170, (1989)
17 Farquharson, S. and Simpson, S. F., “Applications of Raman Spectroscopy to Industrial Processes,” *SPIE*, 1681, 276-290 (1992)
18 Chike, K.E., Myrick, M.L., Lyon, R.E., and Angel, S.M., "Raman and Near-Infrared Studies of an Epoxy Resin," *Applied Spectroscopy*, 47, 10 (1993)
19 Farquharson, S., W. Smith, E. Rigas and D. Granville, “Characterization of polymer composites during autoclave manufacturing by Fourier transform Raman spectroscopy,” *SPIE*, 4201, 103-111 (2001)
20 Zhang, X., Looney, M.G., Solomon, D.H., Whittaker, A.K., *Polymer*, 38, 5835-5848 (1997)
21 Rose, J., R. Osbaldiston, W. Smith, S. Farquharson, and M.T. Shaw, “In-situ monitoring of polymer cure using dynamic rheometry and Raman spectroscopy”, *ANTEC*, 98, 939-944 (1998)
22 Farquharson, S., S. Bhat, R. Osbaldiston, M. DiTaranto, W. Smith, J. Rose, Y-M. Liu, and M.T. Shaw, “Characterization of Polymer Composites by Fiber Optic FT-Raman Spectroscopy,” *SPIE*, 3535, 303-316 (1998)
23 Farquharson, S., W. W. Smith, J. Rose, and M.T. Shaw, " Correlations Between Molecular (Raman) and Macroscopic (Rheology) Data for Process Monitoring of Thermoset Composites", *IFPAC*, 7, 45-53 (2002)
24 Xu, L., J.H. Fu, and J.R. Schlup, "In-situ near infrared spectroscopy of epoxy resin-aromatic amine cure mechanisms", *JACS*, 116, 2821-26 (1994)
25 Dow Chemical (Midland, MI), product literature, form No. 296-224 (1990)